

# Evolution of Mass, Charge, and Angular Momentum in Black Hole Evaporation: a Comparative Analysis

Christopher Ewasiuk and Stefano Profumo

*Department of Physics and Santa Cruz Institute for Particle Physics,  
University of California, Santa Cruz, CA 95064, U.S.A.*

**Abstract**—We present a comprehensive comparative analysis of the evaporation dynamics of Schwarzschild, Kerr, and Reissner-Nordström black holes, focusing on the evolution of their mass, charge, and angular momentum, using detailed calculations of the corresponding Page factors. We investigate the evolution of black holes during the evaporation process, emphasizing how these quantities evolve relative to one another. Our study incorporates the effects of greybody factors, near-extremal conditions, and the introduction of additional particle species beyond the Standard Model. We demonstrate that the addition of particle degrees of freedom may significantly alter the evaporation hierarchy, potentially leading to scenarios in which the effective black hole charge increases during evaporation. Additionally, we examine the impact of Schwinger pair production and of super-radiance on charged, spinning black hole evaporation. These findings offer new insights into the complex interplay between different black hole parameters during evaporation and highlight the importance of considering additional particle species in the process.

## I. INTRODUCTION

Black hole evaporation, driven by Hawking radiation, has been a central topic of interest in theoretical physics since its theoretical discovery. When a black hole emits thermal radiation due to quantum effects near its event horizon, it loses mass, and, depending on its type and initial conditions, additional otherwise classically conserved quantities such as angular momentum and charge [1], [2]. Understanding the dynamics of mass, angular momentum, and charge loss during black hole evaporation has profound implications for quantum mechanics, thermodynamics, and the information paradox. The hierarchy by which black holes “dis-charge” mass, charge, and angular momentum is the topic of the present study.

In this context, Page factors, introduced in Ref. [2], [3], provide a quantitative framework for describing the rates of energy, angular momentum, and charge loss due to Hawking radiation. These factors have been crucial in analyzing the distinct evaporation dynamics of different black hole types, including Schwarzschild, Kerr, and Reissner-Nordström (RN) black holes, under the semi-classical approximation. While the semi-classical framework assumes a fixed background metric with quantum mechanical evolution of matter and radiation fields, it successfully describes the evaporation process of large-enough black holes, where back-reaction effects are negligible [1].

### A. Black Hole Types and Evaporation Mechanisms

Black holes are classified based on their properties of mass ( $M$ ), angular momentum ( $J$ ), and charge ( $Q$ ). The simplest case, the Schwarzschild black hole, is both non-rotating and uncharged. During its evaporation, only mass is

lost through isotropic thermal radiation [2]. Kerr black holes, however, are rotating, and the presence of angular momentum introduces anisotropic emission due to frame-dragging effects, significantly affecting the evaporation dynamics. In contrast, RN black holes are charged but non-rotating, with charge loss occurring preferentially due to the emission of oppositely charged particles [3].

For Kerr black holes, typically angular momentum is lost much faster than mass through the emission of higher-spin particles, leading to a “spin-down” process toward a Schwarzschild-like state [2], [4], [5]. Similarly, in the case of RN black holes, charge is typically dissipated on much shorter timescales than mass, due to the strong, fast emission of charged particles when the latter are thermodynamically available (i.e. when their mass is around, or below, the hole’s temperature) [3], [6]. Both systems, however, exhibit unique pathways of evolution before settling into nearly neutral, non-rotating configurations. Additionally, assumptions on the existence of degrees of freedom beyond the “Standard Model” (SM) of particle physics is crucial to the validity of the pattern described above.

The evaporation process is further modified by greybody factors, which describe deviations from an ideal blackbody spectrum caused by the scattering of radiation in the curved black hole spacetime [7], [8]. These factors play a significant role in determining the emission rates and partitioning of energy across particle types and modes.

### B. Comparative Analysis of Evaporation Dynamics

Although much progress has been made in studying the evaporation dynamics of Schwarzschild, Kerr, and RN black holes independently, a systematic comparative analysis using Page factors across these black hole types is relatively sparse. For instance, studies show that Schwarzschild black holes evaporate the slowest due to their isotropic Hawking radiation [2], [9]. Kerr black holes lose angular momentum several times faster than mass and exhibit superradiance effects that enhance the emission of energy from their ergoregions [4], [9]. RN black holes lose charge rapidly, which suppresses following radiation owing to the Coulomb potential barrier induced by charge [3].

Numerical and analytical results suggest that charged black holes with high charge-to-mass ratios ( $Q/M$ ) exhibit phenomena such as Schwinger pair production and quantum charge fluctuations near their event horizons [8], [6]. In extremal cases (e.g., Kerr or RN black holes near their physical limits), the surface gravity approaches zero, resulting in vanishing thermal emission under the semi-classical approximation, though

quantum corrections modify this behavior [10], [11]. As we discuss below, super-radiance – the accumulation of light bosons effectively orbiting, in a “gravitational atom” guise, the black hole – also leads to anomalously fast shedding of angular momentum for certain combinations of angular momentum and boson-black hole masses.

### C. Motivation and Open Problems

Despite the availability of detailed studies on the evaporation dynamics of specific black hole types, significant gaps remain in comprehensively understanding how mass, angular momentum, and charge evolve comparatively across Schwarzschild, Kerr, and RN black holes. Existing work typically focuses on individual evaporation characteristics or broader formulations of Hawking radiation but often lacks explicit integration of these findings into a unified framework for comparative analysis. Key questions include:

- How do Page factors for energy, angular momentum, and charge loss differ quantitatively across Schwarzschild, Kerr, and RN black holes during evaporation?
- What are the relative timescales for the loss of conserved quantities, and how do greybody factors influence these dynamics?
- How do near-extremal conditions (e.g., high  $a/M$  or  $Q/M$ ) modify the evaporation process for rotating or charged black holes?
- How does the presence of additional degrees of freedom to the standard model of particle physics changes the standard picture?
- What other possible mechanisms can alter the relative loss rates of charge, angular momentum and mass?

In what follows we quantitatively address all of the questions listed above. The structure of the remainder of this study is outlined below. The following section describes the Page factor evolution for light BHs. We outline the general procedure we follow to compute time evolved factors, considering both the spinning and charge evolution of these factors. We also include the effects of additional dark degrees of freedom on parameter dissipation. In Section IV we discuss the results of prior studies, and how the relative dissipation of mass, charge and spin can vary as a result of the introduction of new, additional particles. Next, in Section V we discuss how the time evolution of the various parameters changes under the additional inclusion of Schwinger pair production, which, we will show, can have a significant impact on the time evolution of light, charged BHs. In the final section we discuss how super-radiance and the formation of gravitational atoms affects the extraction of angular momentum and lifetimes for Kerr BHs. The final sec. VII draws our final considerations and concludes. In what follows, we work in natural units where  $G = \hbar = c = 1$ .

## II. PAGE FACTOR EVOLUTION

The evolution of intrinsic BH parameters such as spin and mass can be determined by the so-called Page factors, as outlined in [12]. Generally, the lifetime of a BH scales as the black hole mass to the third power,  $M^3$ , given that

the evaporation rate follows the classical Stefan-Boltzmann equation, and area is proportional to  $R_S^2 \sim M^2$ ,  $R_S$  being the black hole Schwarzschild radius, and  $T_H \sim M^{-1}$ , with  $T_H$  the Hawking temperature; as a result, the scale-invariant Page factor for the BH mass is defined as

$$f(M, x^*) = -M^3 \frac{d \ln(M)}{dt} = -M^2 \frac{dM}{dt} \quad (1)$$

where  $x^*$  corresponds to the intrinsic spin  $a^*$  or charge  $Q^*$ , depending on if we are describing the Kerr or RN metrics. We will use here the effective dimensionless quantities  $a^* = \frac{a}{M} = \frac{J}{M^2}$  and  $Q^* = \frac{Q}{M}$ .

The Page factor for angular momentum is defined as

$$g(M, a^*) = -M^3 \frac{d \ln(J)}{dt} = -\frac{M}{a^*} \frac{dJ}{dt} \quad (2)$$

To describe charge evolution, we define the additional scale-invariant quantity

$$h(M, Q^*) = -M^3 \frac{d \ln(Q)}{dt} = -\frac{M^2}{Q^*} \frac{dQ}{dt}. \quad (3)$$

The rates of particle emission are described as in Ref. [13] and give

$$f(M, x^*) = -M^2 \frac{dM}{dt} = -M^2 \int_0^\infty E \sum_i \frac{d^2 N_i}{dt dE} dE, \quad (4)$$

$$g(M, a^*) = -\frac{M}{a^*} \frac{dJ}{dt} = -\frac{M}{a^*} \int_0^\infty \sum_i g_i \sum_{l,m} \frac{d^2 N_{l,m}}{dt dE} dE, \quad (5)$$

where the terms

$$\frac{d^2 N_{l,m}}{dt dE} = \frac{1}{2\pi} \frac{\Gamma_{s,l,m}(M, E, x^*)}{e^{E/T} - (-1)^{2s}}, \quad (6)$$

$$\frac{d^2 N_i}{dt dE} = g_i \sum_{l,m} \frac{d^2 N_{l,m}}{dt dE} \quad (7)$$

describe the total number of outgoing particles created within the BH horizon, as described in [13]. This leads to an analogous Page factor describing charge evolution from Eq. (3):

$$h(M, Q^*) = -\frac{M^2}{Q^*} \frac{dQ}{dt} = -\frac{M^2}{Q^*} \int_0^\infty \sum_i q_i g_i \sum_{l,m} \frac{d^2 N_{l,m}}{dt dE} dE. \quad (8)$$

The terms  $q_i$  are the individual particle charge and  $g_i$  are available particle degrees of freedom. Note that the term  $h(M, Q^*)$  does not include a double counting of the number of degrees of freedom from including antiparticles, as antiparticles and particles included would have opposite charge. We define the effective charge as being from 0 to 1, as the process for shedding negative charge is identical to the scenario of shedding positive charge aside from a sign change.

The computations in the following section are done using *BlackHawk* [14] for the Kerr metric. However, *BlackHawk* does not account for time evolution of a RN BH and new proprietary code was written to overcome this issue. In our consideration of the charged metric, we have adopted the

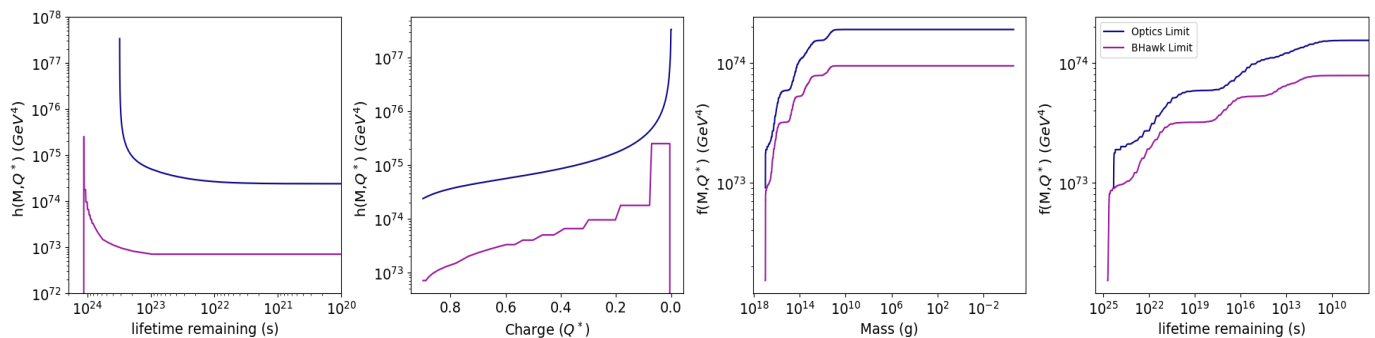


Fig. 1. Comparison of the output of the *BlackHawk* code and our use of the Geometric Optics approximation for  $h(M, Q^*)$  and  $f(M, Q^*)$ . All panels show BHs with masses  $10^{17}$ g and effective charge  $Q^* = 0.9$

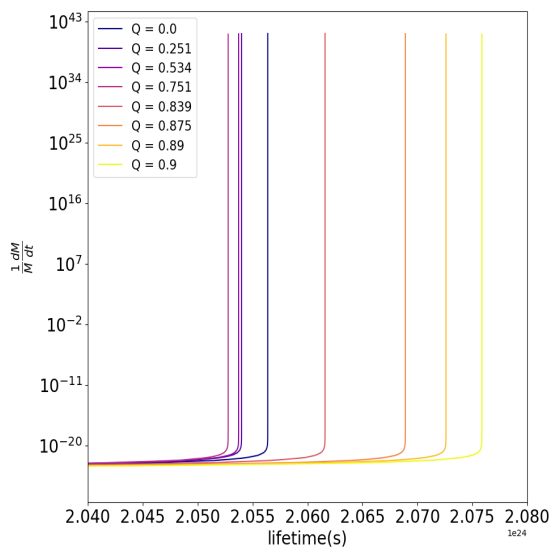


Fig. 2. Lognormalized mass loss rates as a function of lifetime for different effective charge. Increasing effective charge lowers the overall temperature of the BH, slowing particle emission. The initial BH mass is set at  $10^{17}$  g as larger masses will not change the initial mass loss rate.

optical limit approximation to compute the particleless greybody factor:

$$\Gamma = 27M^2 E^2, \quad (9)$$

where  $E$  is the total energy of the emitted particle, taken to be extremely large in comparison to an individual particles rest mass. The accuracy of this approximation, in comparison to the page factors computed for a charged BH within *BlackHawk*, is shown in Fig. 1. Specifically, the plots in Fig. 1 offer a direct comparison between our geometric optics approximation and *BlackHawk*. In this comparison we find an order of magnitude lifetime shortening, as seen in the leftmost plot within Fig. 1. This approximation also illustrates the small differences in our computed Page factors, shown in the remaining plots of Fig. 1. The Page factor  $f(M, Q^*)$  is seen to exhibit step-like increases. These sudden increases followed by a plateau are instances in a BHs lifetime where the emission of a massive particle transitions from being unlikely to probable. While our code is an an apparent overestimation

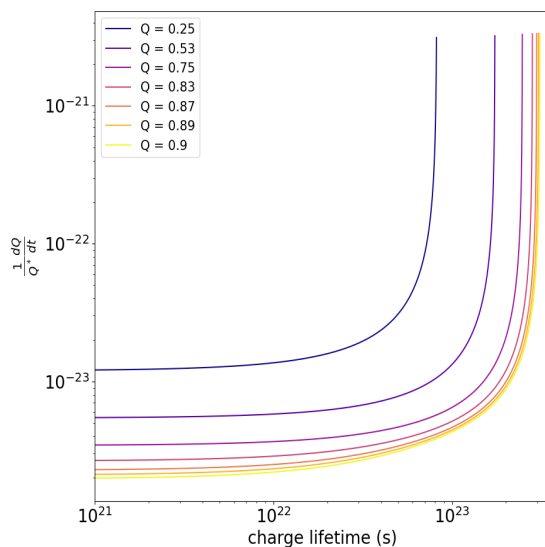


Fig. 3. Charge loss rate due to Hawking radiation for various spins normalized by the initial effective charge  $Q^*$  of a BH.

in comparison to *BlackHawk*, it offers a look into the general behavior of a RN BH under the addition of a large number of degrees of freedom.

### III. EFFECT OF A LARGE DARK SECTOR ON PARAMETER EVAPORATION

Introducing a dark sector containing a large number of degrees of freedom results in significant changes in the evolution of charged or rotating BHs. Given  $a^* = \frac{J}{M^2}$  and  $Q^* = \frac{Q}{M}$ . An effective spin or charge equal to 1 corresponds to extremality where evaporation shuts off. The total number of particles needed to neutralize a charged black hole are of order  $M$ , whereas the number needed to carry off overall angular momenta  $J$  scales as  $M^2$ . Therefore the standard hierarchy of parameter loss, when considering purely evaporative processes, begins with charge neutralization, followed by loss of spin and finally mass evaporation which, as noted above, scales as  $M^{-2}$ . However, we are interested in possible scenarios that perturb this hierarchy, and in analyzing the ensuing patterns. Beginning with charged BH evolution, we consider the case where we add an additional dark sector comprising charged particles to the SM.

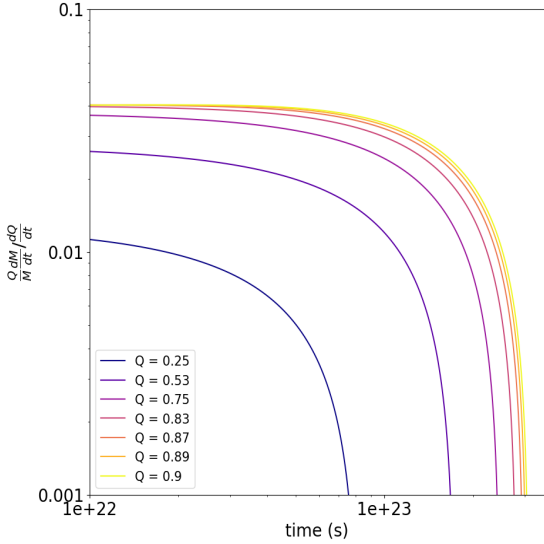


Fig. 4. Lines of  $\frac{1}{Q^*} \frac{dM/dt}{dQ^*/dt}$  lognormalized for a RN BH for various effective charge values. Initial conditions are for a  $M = 10^{17}g$  BH and no included DM.

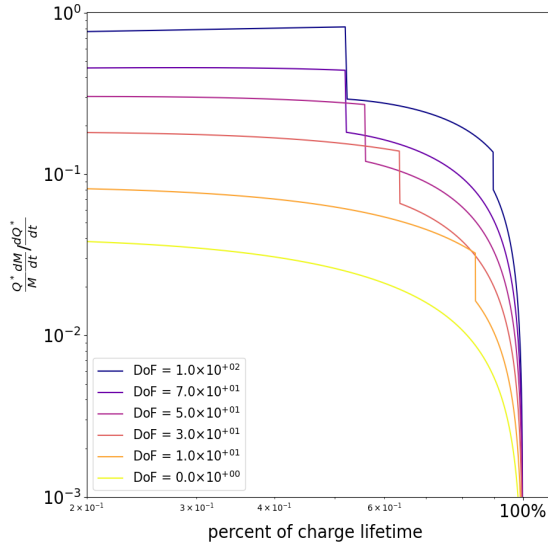


Fig. 5. Illustration of the effects of adding spinless, chargeless DM to the BH evaporation spectrum while varying the number of degrees of freedom. Initial conditions are for a BH with mass  $10^{17}g$ , effective charge  $Q^* = 0.9$  and introduced dark matter with  $m_{DM} = 0$  GeV. Adding larger degrees of freedom will result in a transition from a regime where  $\frac{1}{Q} \frac{dQ}{dt}$  is dominant to a regime where  $\frac{1}{M} \frac{dM}{dt}$  begins to dominate. Such a transition is illustrated for the same initial parameters in Fig. 6, and occurs when the lines reach a maximum of 1. Illustration only shows rates when the BH is considered charged, afterwards the BH is considered static.

### A. Reissner-Nordström Evaporation Rates

The overall effective charge of a BH will shrink both the horizon and Cauchy radii via

$$r_{\pm} = r_{H,C} = r_S \frac{1 \pm \sqrt{1 - Q^{*2}}}{2}, \quad (10)$$

where  $r_S = 2M$ . This affects the BH temperature and therefore the emission spectrum, which is defined as

$$T_{RN} = \frac{r_+ - r_-}{4\pi r_+^2}. \quad (11)$$

As temperature is raised, the overall probability to release a particle of specific rest mass energy is raised, as seen in the temperature dependence of Eq. (6). We can see how larger effective charge results in significantly larger lifetimes for the same mass in Fig 2. This is due to increased effective charge lowering the BH temperature, again reducing particle emission probability. Increasing effective charge also increases the charge loss rate, yet the rate normalized by the effective charge shows that BHs with lower charges shed charge relatively more efficiently. This can be seen in both Fig. 3 and Fig. 4 and is the reason that BHs with larger overall charge shed charge on a longer timescale. In both plots we see that for BHs light enough to emit electrons that the charge loss rate dominates over the mass loss rate.

Ultimately, we are interested in the rate of mass loss compared to the rate of charge loss. The ratio  $\frac{1}{Q^*} \frac{dM/dt}{dQ^*/dt}$  allows us to look at the time evolution of both parameters on a normalized scale. We can express the denominator of this ratio by taking the total derivative of  $Q^* = \frac{Q}{M}$  as:

$$\frac{dQ^*}{dt} = \frac{1}{M} \frac{dQ}{dt} - \frac{Q^*}{M} \frac{dM}{dt} \quad (12)$$

in terms of the page factors, this is:

$$\frac{dQ^*}{dt} = Q^* \frac{f(M, Q^*) - h(M, Q^*)}{M^3}, \quad (13)$$

where the relevant page factors are defined in Eqs (4), (8). If the number of additional degrees of freedom is small enough such that  $\frac{dQ^*}{dt}$  remains negative, the BH is free to fully evaporate. The effect of including both massless DM with varying degrees of freedom can be seen in Fig. 5. This plot can be interpreted as having an initial constant value of  $\frac{dQ}{dt}$  for each line while the term  $\frac{dM}{dt}$  grows due to the introduced DM. At later stages of the BHs lifetime, more charged particles are emitted, resulting in an increased  $\frac{dQ}{dt}$  and dropoff of the lognormalized ratio. Note that in the previous line we refer to the true charge loss rate ( $\frac{dQ}{dt}$ ) of the BH remaining constant rather than effective charge rate ( $\frac{dQ^*}{dt}$ ). For the values considered, the log-normalized ratio  $\frac{Q^*}{M} \frac{dM/dt}{dQ^*/dt}$  approaches 1 and are where the normalized loss rates approach the same values. Initially we have a scenario where the charge loss  $\frac{dQ}{dt}$  is approximately the same magnitude as mass loss, and causes the effective charge  $Q^*$  to plateau and remain approximately constant until more charged particles can be emitted. In the figure we see effective charge begin to dominate at later times when charge is nonzero. In this case, charge loss will eventually exceed mass loss and the BH will discharge well before all the BHs mass is evaporated.

Once  $\frac{dM}{dt}$  approaches the charge loss rate  $\frac{dQ^*}{dt}$ , one can continue to add a larger number of degrees of freedom to our model. For extremely large numbers of additional degrees of freedom, this results in a dominant  $\frac{dM}{dt}$  term in comparison to  $\frac{dQ^*}{dt}$ , or values of  $f(M, Q^*)$  greater than values of  $h(M, Q^*)$ .

Using Eq (12), we can see that this should create an effective charge loss rate of

$$\frac{dQ^*}{dt} \approx -\frac{Q^*}{M} \frac{dM}{dt} \quad (14)$$

in the limit where  $\frac{dM}{dt} \gg \frac{dQ^*}{dt}$ . The ratio of  $\frac{\frac{1}{M} \frac{dM}{dt}}{\frac{1}{Q^*} \frac{dQ^*}{dt}}$  will then effectively become:

$$\frac{\frac{1}{M} \frac{dM}{dt}}{\frac{1}{Q^*} \frac{dQ^*}{dt}} = \frac{\frac{1}{M} \frac{dM}{dt}}{\frac{1}{Q^*} \left(-\frac{Q^*}{M} \frac{dM}{dt}\right)} = -1 \quad (15)$$

for large values of  $\frac{dM}{dt}$ . This effect can be seen within Fig. 6, where the values for  $\frac{dQ^*}{dt}$  transition from negative to positive. This causes the effective charge of the BH to increase after the introduction of a large number of new, non-charged degrees of freedom. For introduced degrees of freedom that allow  $f(M, Q^*)$  to become comparable to  $h(M, Q^*)$ , the effective charge neutralization of the BH stagnates and both true charge and mass evaporate at comparable rates. We can imagine this scenario through Eq. (12), when the term  $\frac{1}{M} \frac{dM}{dt}$  equals the term  $\frac{Q^*}{M} \frac{dM}{dt}$ , making the effective charge loss rate zero for select introduced degrees of freedom. For a BH of mass  $10^{17}$ g, we estimate that number of massless degrees of freedom required hovers between roughly  $220 \leq N_{doF} \leq 270$  and can be seen in Fig. 6. The number of degrees of freedom required for this transition is BH mass dependent, again seen through Eq. (12). Any introduced number of degrees of freedom larger than this, for a given BH mass, will result in a scenario where the effective charge of the BH will increase. This upsets the traditional hierarchy where charge will be evaporated away first. Varying the mass of the included dark matter serves to increase the BH lifetime; i.e. as the mass of the dark matter increases, the temperature threshold for dark matter evaporation increases, resulting in a longer duration spent radiating non-DM particles.

In this setup we have considered relatively light BHs ( $M \approx 10^{17}$ g) that allow for significant emission of massive particles. For smaller black hole masses, the Hawking temperature is high, allowing the emission of increasingly massive particles as the black hole continues to evaporate. This leads to a rapid broadening of the emission spectrum, with heavier and heavier particles becoming kinematically accessible in quick succession. In contrast, the temperature for larger black hole masses is much lower, restricting emission primarily to the lightest or massless particles, such as photons and neutrinos, with heavier particles being exponentially suppressed. In fact, the majority of the lifetime for heavier BHs will be spent radiating massless degrees of freedom. In the standard model this amounts to blackbody radiation and serves to only decrease mass. When much heavier charged BHs are considered we obtain a scenario where it becomes impossible to radiate charge via the standard evaporative processes. Since we have a decreasing mass and a stagnating charge, the overall effective charge of a BH,  $Q^* = \frac{Q}{M}$ , begins to increase and approach a extremal BH for all BH masses greater than roughly  $10^{17}$ g. The general increasing of effective charge for a BH mass of  $10^5 M_\odot$  or  $1.9885 \times 10^{38}$ g can be seen in Fig. 7. This effect also increases the lifetime of the BH indefinitely. The increase

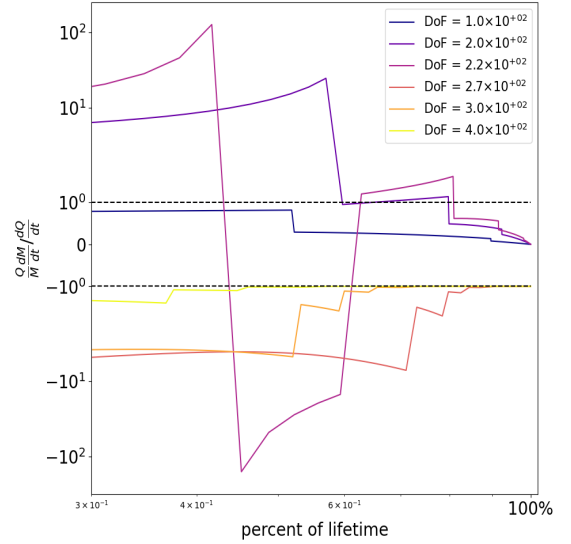


Fig. 6. Lognormalized ratio of mass and charge loss for chargeless degrees of freedom starting when mass loss dominates and transitioning to a region where effective charge loss dominates. Effective charge loss rates close to zero result in the numerical divergences, and are moments when charge loss rates match mass loss rates.

of effective charge lowers the BH temperature, suppressing the mass loss page factor  $f(M, Q^*)$ . The end result is effectively an extremal black hole with a suppressed mass and charge loss and a Hawking temperature that approaches zero, stopping any evaporative processes. We will see later that the tendency for a BH to approach more extremal is negated when we include the effects of Schwinger pair production. The inclusion of this effect in addition to Hawking radiation is talked about in more detail within Section V.

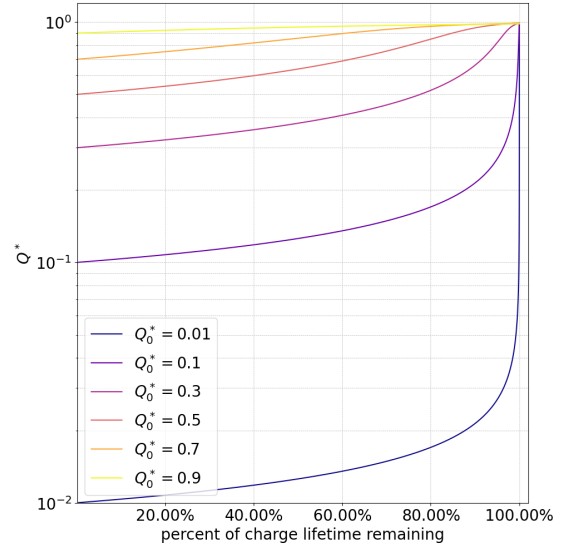


Fig. 7. Effective charge as a function of lifetime for a  $10^5 M_\odot$  BH. Charged particles are exponentially suppressed for the majority of heavy BHs lifetimes while mass is able to evaporates via photon emission. Effective charge therefore strictly increases until it becomes a extremal BH, at which point the temperature approaches zero and evaporation stops.

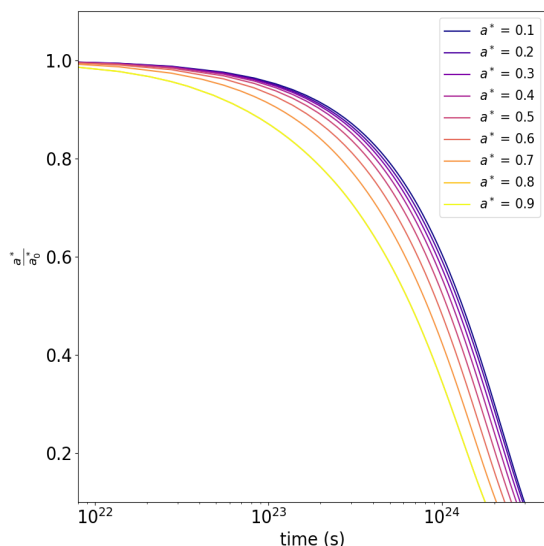


Fig. 8. Overlay of varying effective spin normalized by initial spin value as a function time for a Kerr BH. Lifetime is given for a Kerr BH of mass  $1e17g$ , and introduced DM is not considered.

### B. Kerr Evaporation Rates

We consider here BHs with intrinsic angular momentum  $J$  instead. The parameter describing the evolution of a BH with respect to its angular momentum  $J$  is the effective spin parameter  $a^*$ . Similarly to Eq. (13), we can find the effective spin loss rate

$$\frac{da^*}{dt} = \frac{1}{M^2} \frac{dJ}{dt} - 2 \frac{J}{M^3} \frac{dM}{dt} \quad (16)$$

In terms of Page factors defined in Eq.s (4), (5), this is

$$\frac{da^*}{dt} = a^* \frac{2f(M, a^*) - g(M, a^*)}{M^3} \quad (17)$$

which will dictate the evaporation of spin for a Kerr BH.

Contrary to the case of shedding charge, there is no scenario in which an emitted particle always carries zero angular momentum away from the black hole. In the case of charge loss, the black hole can, in principle, emit a neutral particle, meaning that not every emission necessarily contributes to charge depletion. However, for angular momentum, any emitted particle must carry away some amount of total angular momentum, ensuring that the black hole's angular momentum is always being affected by its radiation. Even if we consider a particle with a quantum spin number of zero (such as a scalar boson), the total angular momentum  $J$  of the emitted particle is given by the sum of its intrinsic spin  $S$  and its orbital angular momentum  $L$ ,

$$J = L + S \quad (18)$$

For a spinless particle,  $S = 0$ , but the emitted particle will still have some nonzero orbital angular momentum  $L$ . Since angular momentum is quantized, even the lowest possible allowed orbital angular momentum state for a given emission process is nonzero, particularly when considering emissions from a rotating body. This results in a scenario where  $g(M, a^*)$  will always be greater than  $2f(M, a^*)$  for all greybody factors

tabulated. Therefore, spin will always be shed before mass and will cause a BH to tend away from an extremal BH for all particles considered. Still, we can compare timescales of effective spin loss against the charge loss values obtained above. Looking at Fig. 8, we can see that the timescale for spin evaporation for a maximally spinning ( $a^* = 0.9$ ),  $10^{17}$  g mass BH is  $\approx 1.8 \times 10^{24}$  seconds. Compared to the charge lifetime of  $\approx 3 \times 10^{23}$  seconds, we find that spin is shed approximately 6 times slower in our analysis. Again, it is important to emphasize that our lifetime results for charge are an overestimation, however, the hierarchy coincides with what is to be expected.

We have also investigated the effects of introducing massless particles of varying degrees of freedom and spin on shedding angular momenta. The results can be seen in Fig. 9. The most interesting case is the far left panel, where we have considered spin zero particles. In this case, the overall spin carried away by the particle is entirely orbital angular momentum. While the page factor for spin  $g(M, a^*)$  is always larger than the mass loss term  $2f(M, a^*)$ , in this case the difference between the two becomes very small. This results in the denominator term  $\frac{da^*}{dt}$  in the lognormalized ratio illustrated on the figure's y-axis to become extremely small in comparison to the mass loss term  $\frac{dM}{dt}$ . For all other cases the intrinsic spin  $S$  of the particle acts to increase the spin loss term, resulting in a lognormalized ratio less than 1. We see apparent divergences in the spin zero case near the end of the spin lifetime of the BH due to the presence of a scalar particle with large number of degrees of freedom. Since  $\frac{da^*}{dt}$  has a much weaker dependence on a scalar particle than the nonzero spin cases considered, when effective spin approaches zero the mass loss rate begins to dominate. The stronger dependence of  $\frac{da^*}{dt}$  on particle spin  $S$  will cause an effective suppression of this effect in the cases of nonzero spin, as both mass loss rate and spin loss rate will be directly dependent on this large sector of introduced degrees of freedom.

We have also illustrated how effective spin affects the lognormalized ratio  $\frac{a^*}{M} \frac{dM/dt}{da^*/dt}$  in the absence of a large number of introduced degrees of freedom in Fig. 10. Again the lognormalized ratio expressed in the figure shows how the normalized mass loss and spin loss rates compare. Values greater than 1 illustrate regions where mass is shed faster than spin, and values less than 1 represent the inverse. In Fig. 10, the plot describes how as effective spin of a BH is increased the spin loss rate is decreased in comparison to the mass loss rate. Again this is a result of the dependence of a Kerr BHs temperature on the effective spin of the BH. As effective spin increases the overall BH temperature decreases, resulting in delayed particle evaporation thresholds and a higher exponential suppression of evaporated particles in comparison to lower effective spins. As we approach the end of a BHs lifetime the spin loss term begins to dominate until spin is completely shed.

## IV. RELATIVE HIERARCHIES

The purpose of the section above is to illustrate the possibility of upsetting the hierarchy of charge, spin and mass loss

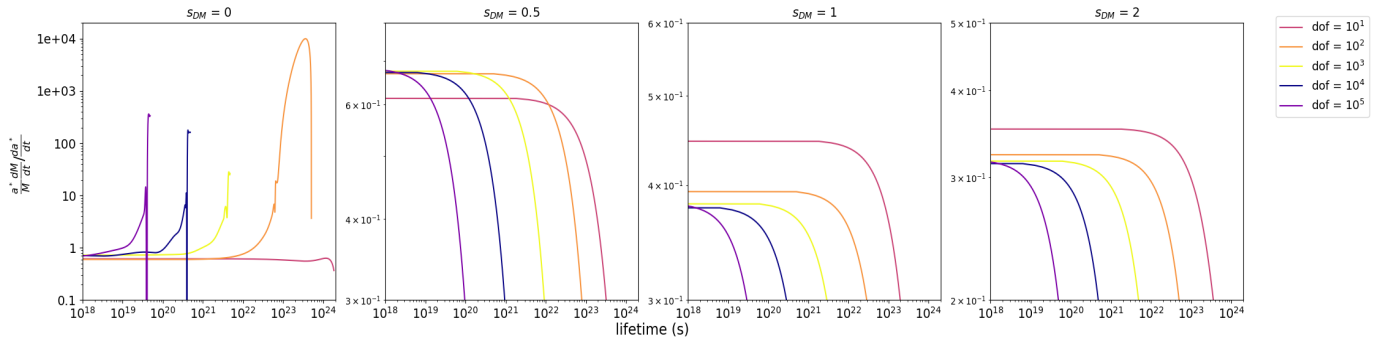


Fig. 9. Effect of adding various spin dark matter with various masses to the evaporation model of a Kerr BH. BH initial parameters are  $a^* = 0.8$ ,  $m_{BH} = 10^{17}g$ .

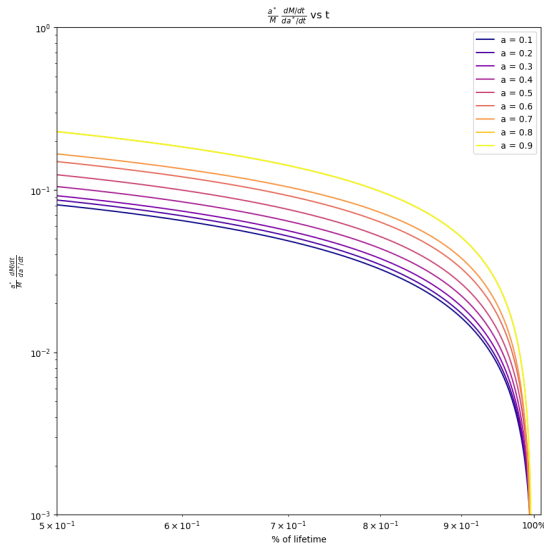


Fig. 10. Lines of  $\frac{1}{M} \frac{dM}{dt} / \frac{1}{a^*} \frac{da^*}{dt}$  lognormalized for a Kerr BH for various effective spin values.

as dictated by the standard model. Our findings indicate that under any circumstances, spin is lost before mass. However, we have found that through the introduction of a large number of massive or massless degrees of freedom we can create a scenario where we can increase the effective charge of a RN BH. The standard hierarchy we set out to upset is as follows; charge is neutralized first, followed by spin and finally mass will be depleted ( $\frac{dM}{dt} < \frac{dJ}{dt} < \frac{dQ}{dt}$ ). There are two distinct ways in which we can upset this natural order.

The first possibility of changing the order of parameters lost is through the introduction of a select number of chargeless degrees of freedom. In our consideration of a BH of mass  $M = 10^{17}g$ , if we include massless scalar degrees of freedom within the range of  $100 \lesssim N_{dof} \lesssim 220$ , we find a scenario where the hierarchy changes and spin is shed first, followed by charge neutralization and then finally mass loss ( $\frac{dM}{dt} < \frac{dQ}{dt} < \frac{dJ}{dt}$ ): Since the introduction of chargeless degrees of freedom has no effect on the rate of charge loss, this introduction solely effects the rates of mass and charge loss. Degrees of freedom larger than  $\approx 220$  result in increasing effective charge, and would make mass evaporate faster than

charge. However, degrees of freedom greater than  $\approx 100$  will result in spin being lost faster than charge being lost. Again this is a direct result of these introduced degrees of freedom always being able to carry away some nonzero amount of angular momentum. Again, the upper limit of the number of degrees of freedom is set by the BH mass and can be seen in the dependence of  $\frac{dQ^*}{dt}$  on  $M$  in Eq. (12). The lower limit is also dependent on the intrinsic spin  $S$  of the introduced particle. Higher particle spins will require lower degrees of freedom due to the dependence of the intrinsic spin  $S$  in the total angular momentum  $J$  carried away from the BH. Lower limits can be extracted by looking at degrees of freedom in Fig 9 the result in Kerr lifetimes lower than  $\approx 3 \times 10^{23}$  seconds for specific intrinsic spins. Again as a BH gets heavier the emission spectrum gets exponentially suppressed. So the upper limit will change for select BH masses as well.

The second possibility is when we consider degrees of freedom higher than  $\approx 220$ . In this scenario, we find that the effective charge increases for a  $M = 10^{17}g$  BH. While the overall charge of the BH goes down, it is outpaced by mass. In this scenario we find that again spin is lost first, but we have the order of mass and charge loss reversed in comparison to the first scenario ( $\frac{dQ}{dt} < \frac{dM}{dt} < \frac{dJ}{dt}$ ).

Note, again, that in the absence of Schwinger pair production extremely massive BHs act similar to blackbodies. In this case, even without the addition of any dark degrees of freedom, we have a scenario where the BH evaporates a significant portion of mass before having any noticeable amount of charge evaporated. Since any charged particle within the standard model has some nonzero mass, the production of such particles will be exponentially suppressed for the majority of the BHs lifetime. Once the BH reaches a mass of roughly  $10^{17}g$ , it begins to emit a significant amount of charged particles. before that point we find that the effective charge will increase and approach a extremal charged BH. For the majority of the lifetime of a BH, effective charge increases until charged particles can be produced. While this isn't necessarily upsetting the natural hierarchy discussed above since charge is eventually dissipated before mass near the end of the BHs lifetime, the majority of the lifetime is naturally spent increasing the effective charge for heavier BHs.

## V. A CHARGED CAVEAT: SCHWINGER PAIR PRODUCTION

The above analysis for a RN BH only considers the production of charged particles through the computation of their greybody factors outlined in [14]. We did not consider, however, purely classical processes that could neutralize the BH. For example, if the BH were surrounded by charged interstellar media, we would see a fairly quick neutralization of the charge due to selective accretion of particles with charge opposite the BH. Still, even in the absence of such media we can still have an enhanced charge neutralization through quantum effects. A possible significant contribution comes from the Schwinger effect [15], [16], [17]. The Schwinger effect describes spontaneous pair creation of charged particles in the presence of an extremely strong electric field. In the majority of electric fields the production is exponentially suppressed, yet for electric fields higher than the threshold field this effect can become dominant. Such a strong field results in vacuum decay and the following creation of electron-positron pairs. One of the created particles will experience a large repulsive force, while the other is attracted towards the center of the BH. The particle escaping to infinity will carry off a charge  $e^{+/-}$ , while the attracted particle neutralizes an additional equivalent charge by falling into the horizon. This process serves to lower the charge of the field by  $2e$  for each pair created [15] [18]. The greybody factors for electron and positron production can then be significantly enhanced via Schwinger pair production.

Schwinger pair production falls under the umbrella of Hawking radiation. While we will treat the production of charged particles separately from the thermal Hawking flux of neutral particles, it should be remembered that they are actually all part of the Hawking radiation; the charged-particle creation is described (thermodynamically) by a nonzero chemical potential associated with the black-hole electromagnetic field [18], but has been neglected in our initial analysis due to the different mechanism for which the charged particles are produced. We can estimate the effect that this has on the charge lifetime of a RN BH by modifying Eq. (12). Starting with the Schwinger pair production formula [18], the electron-positron creation rate per unit volume is

$$\Gamma = \frac{e^2}{4\pi^3} \frac{Q^2}{r_+^4} \exp\left(-\frac{\pi m_e^2 r_+^2}{eQ}\right) \quad (19)$$

where  $m_e$  is the mass of the electron and  $Q$  is the BH charge defined as  $Q = Q^* M$ . We will require that the term  $\frac{e^3 Q}{m_e^2 r_+^2} \ll 1$  and consider only the leading order term. If this assumption is violated the series is no longer convergent and can be assumed to approach infinity, resulting in a massive discharge of the RN BH until the effective charge is low enough to allow the condition to be satisfied. The charge loss rate per unit time is then

$$\frac{dQ_S}{dt} = -2e \int \Gamma dV \quad (20)$$

where  $Q_S$  has been introduced to denote the difference between charge loss specifically due to Schwinger pair production. Integrating Eq. 19 rate per unit volume we find the

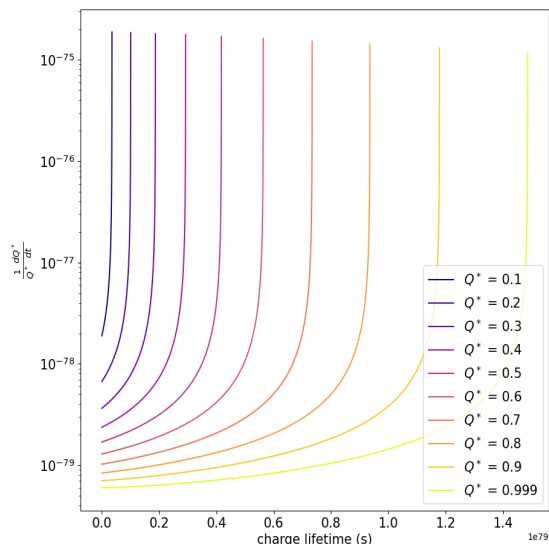


Fig. 11. Effect of Schwinger pair production on  $\frac{dQ^*}{dt}$  for various effective charges for a BH of initial mass  $M = 10^4 M_\odot$ . All charge is lost before any significant amount of mass is lost.

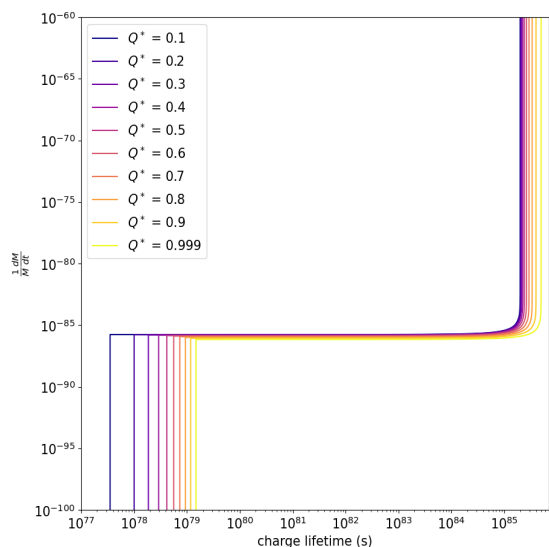


Fig. 12. Effect of Schwinger pair production of  $\frac{dM}{dt}$  for various effective charges. BH has initial mass  $M = 10^4 M_\odot$ . Sudden jump on the left hand side of the plot is when charge is neutralized. From then on BH behaves as if static.

charge loss rate to be

$$\frac{dQ_S}{dt} = \frac{-e^3}{\pi^2} \frac{1}{r_+} \exp\left[-\frac{r_+^2}{QQ_0}\right] - \frac{\pi}{(QQ_0)^{1/2}} \operatorname{erfc}\left[\frac{r_+}{(QQ_0)^{1/2}}\right]. \quad (21)$$

where  $\operatorname{erfc}(x)$  is the complementary error function and  $Q_0 = \frac{e}{\pi m_e^2}$ . The effective charge loss in Eq (12) becomes

$$\frac{dQ^*}{dt} = \frac{1}{M} \frac{dQ}{dt} + \frac{1}{M} \frac{dQ_S}{dt} - \frac{Q^*}{M} \frac{dM}{dt} \quad (22)$$

where  $\frac{dQ}{dt}$  describes the charge particle production at the horizon due to quantum vacuum fluctuations and  $\frac{dQ_S}{dt}$  describes electron-positron production due to the presence of a large electric field. The rapid discharge due to Schwinger pair

production would also affect the mass loss rate  $\frac{dM}{dt}$  as well. The mass loss rate can be obtained by looking at

$$\frac{dM}{dt} = \frac{\partial M}{\partial Q} \frac{\partial Q}{\partial t} = \frac{\partial M}{\partial r_+} \frac{\partial r_+}{\partial Q} \frac{\partial Q}{\partial t} \quad (23)$$

Working out the algebra we have the expression

$$\frac{dM_S}{dt} = \frac{Q^* M}{r_+} \frac{dQ_S}{dt} \quad (24)$$

which is analogous to the result from [18] in natural units. This additional term will serve to speed up the mass loss rate for a charged BH as long as  $\frac{dQ_S}{dt}$  is nonzero.

We can calculate an order of magnitude estimate to see if this effect will have a significant impact on the discharging of a RN BH. Both the Schwinger and the Hawking discharge rate feature an exponential suppression; in the case of the Schwinger discharge rate this is (Note that this is the discharge rate per unit volume and the hawking rate is per unit energy)

$$\Gamma_{\text{Sch}} \sim \exp\left(-\frac{\pi m_e^2 r_+^2}{eQ}\right), \quad (25)$$

with

$$r_+ = M \left(1 + \sqrt{1 + (Q/M)^2}\right)$$

and  $e$  the electron charge; expressing the above in natural units, neglecting order 1 factors, we get

$$\Gamma_{\text{Sch}} \sim \exp\left(-\frac{m_e^2 M^2}{eQ}\right). \quad (26)$$

The Hawking evaporation rate is Boltzmann suppressed by  $m_e/T_H$ , where

$$T_H \sim \frac{1}{M} \left(1 - \frac{Q^2}{M^2}\right),$$

thus

$$\Gamma_{\text{Hawk}} \sim \exp\left(-\frac{M m_e}{1 - \frac{Q^2}{M^2}}\right). \quad (27)$$

The Schwinger discharge rate dominates when

$$\Gamma_{\text{Sch}} \gtrsim \Gamma_{\text{Hawk}} \Rightarrow \frac{m_e^2 M^2}{eQ} \lesssim \frac{m_e M}{\left(1 - \frac{Q^2}{M^2}\right)}. \quad (28)$$

Rearranging, I find that in terms of mass-to-charge ratio  $x_e = (e/m_e)$  and  $x_{\text{BH}} = Q/M$ , Schwinger discharge dominates if

$$\frac{1 - x_{\text{BH}}}{x_{\text{BH}}} \lesssim x_e \simeq 6.4 \times 10^{21}. \quad (29)$$

In turn, this implies

$$x_{\text{BH}} \gtrsim 10^{-22} \quad (30)$$

Since the Planck charge is  $11.7e$ , I find that Schwinger discharge dominates for any black hole with any electric charge  $Q \geq e$  when  $M \leq 10^{18}$  grams

Looking at Fig 11, we can see the how Schwinger pair production enhances number of charged particles in the Hawking spectra. In this case we have considered a much larger BH ( $10^4 M_\odot$ ). The primary purpose of this choice is to consider a stage in a charged BHs life when there is essentially only blackbody radiation. This mechanism only serves to deplete

mass from a charged BH and, by Eq (12), would serve to increase the overall effective charge of such a large BH. Without Schwinger pair production, there would be a tendency for charged BHs to approach extremality in all scenarios. However, we can see that this effect serves to rapidly discharge the BH in comparison to the mass loss timescales. Looking at figure 12, we can see that the lifetime of a BH with various effective charges hovers around  $10^{85}$ s for BH of this size. This is roughly  $10^{16}$  times larger than the timescale for which a BH will discharge due to Schwinger pair production. Its important to note that this analysis only includes effects from the leading order term for Schwinger production and therefore indicates the largest lifetimes possible when including this effect. All higher order terms serve to increase the electron-positron production rate, and therefore will decrease the lifetime of a charged BH.

## VI. SUPERRADIANCE AND SPIN: ANGULAR MOMENTUM EXTRACTION

Recent works in BH superradiance also allow for the removal of angular momentum from a BH on shorter timescales than Hawking radiation [19]. While the entirety of the BHs angular momentum can never be fully extracted, the majority can and so will be considered alongside our Hawking analysis for the Kerr metric. Superradiance within a BH is allowed to occur due to the presence of the ergoregion between the two horizons. Within this region, negative energy objects are allowed to exist [20]. The basic mechanic was first proposed as the following thought experiment. We can consider a particle of incoming energy  $E_0$  entering the ergosphere and decaying into two particles. Since we are inside the ergosphere, we can imagine one of the particles decaying into one with negative energy  $E_1 < 0$ . By conservation of energy we obtain the following relation for the energy of the second particle:  $E_2 = E_0 - E_1$  or  $E_2 > E_0$  due to the negative energy particle. The positive energy particle is allowed to then leave the ergoregion, leaving behind a particle of negative energy to ultimately reduce the overall energy of the BH system. Superradance is this phenomenon as a positive feedback loop; extracting energy from the system in the form of an ever increasing number of scalar particles just outside the BH horizon. Due to the presence of the  $\frac{1}{r}$  gravitational potential, the produced scalar particles settle into bound states that closely resemble that of the hydrogen wavefunctions, earning the proposed system the title of a 'Gravitational Atom'. In the following section we will outline the timescales associated the possibility of removing angular momentum from the system via the introduction of massive scalar bosons and the superradiant effect.

Superradiance of a BH is allowed so long as the superradiant condition [19]:

$$\omega < m\Omega_+ \quad (31)$$

is satisfied. In the above equation  $\omega$  refers to the frequency of the incoming scalar wave,  $m$  the azimuthal quantum number of a given state and  $\Omega_+$  the angular velocity of the BH horizon. In general, we assume the population of states occurs

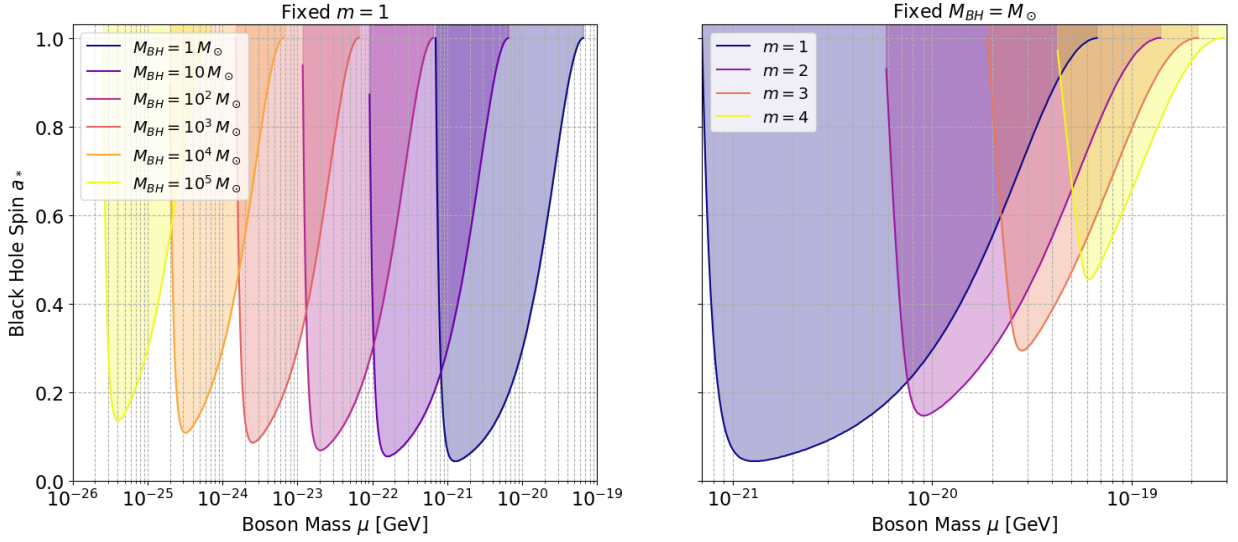


Fig. 13. Parameter space for possible superradiance regions for a given black hole mass and light boson.

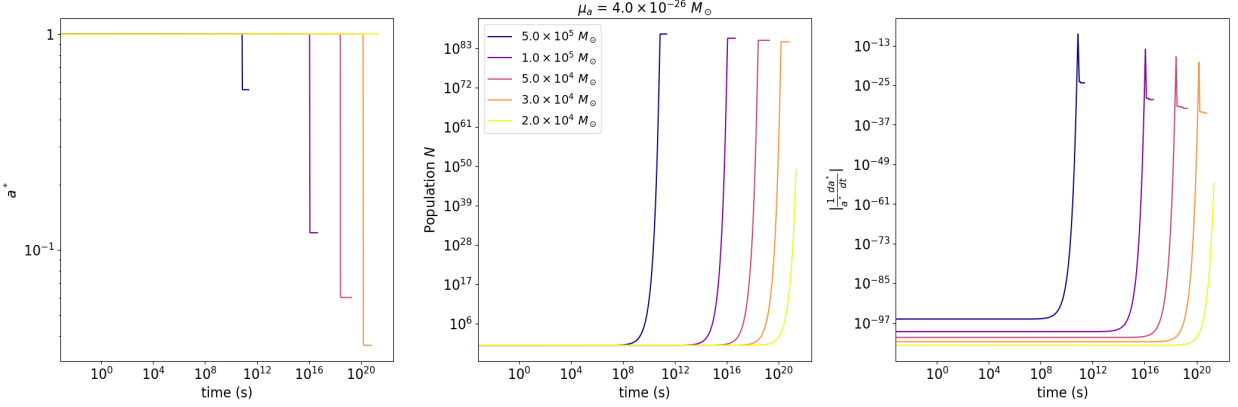


Fig. 14. Effective spin loss due to superradiance of a Kerr BH. Extracting the majority of spin ( $\mathcal{O}(0.1)$  remaining) occurs in approximately  $10^{16}$  s in comparison to the Hawking lifetime for Kerr BHs of  $1.8 \times 10^{24}$  s.

with  $\omega$  to be roughly the boson mass  $\omega \approx \mu_a$ . The overall angular momentum available to be extracted via superradiance is then proportional to the number of particles produced by this process. For each particle extracted from a given BH, the overall angular momentum of the BH is lowered by  $\Delta J = m$ , or an integer quanta of angular momentum proportional to the given state occupied. Therefore, the overall rate of angular momentum extraction from the BH is equivalent to the rate at which superradiance occurs  $\Gamma_{SR}$  for a given particle multiplied by the number of particles of a given state  $N_m$ :

$$\frac{dJ}{dt} = -m\Gamma_{SR}N_m \quad (32)$$

Again using Eq. (16), we estimate the change in effective spin as long as we have the mass loss rate due to superradiance. The mass loss rate of the BH is obtained in a similar manner, except we can replace the quanta of spin  $m$  by the scalar particle mass  $\mu_a$  to get

$$\frac{dM}{dt} = -\mu_a\Gamma_{SR}N_m. \quad (33)$$

All together, the expression for effective spin loss due to superradiance is given by;

$$\frac{da_{SR}^*}{dt} = -\frac{1}{M^2}m\Gamma_{SR}N_m + 2\frac{a^*}{M}\mu_a\Gamma_{SR}N_m. \quad (34)$$

Which is expected to be valid so long as the superradiance condition in Eq. (31) is satisfied and the superradiance rate  $\Gamma_{SR}$  is faster than the Eddington accretion time. We have simulated the effective spin available to be extracted from the BH in the Regge trajectory plots in Fig. V. For any BH mass we can see that, for quantum numbers  $\{n, l, m\}$ , the  $m = 1$  state allows for the largest  $\Delta a^* = a_i - a_f$  in the right hand panel. Additionally, we simulate the parameter space for various BH and scalar boson masses that allow for superradiance. We can see as a general trend that as BH mass increases then overall spin available for extraction decreases. Additionally, we expect that constraints on light boson candidates to be another limiting factor in the possibility of this SR regime being reached for heavy BHs. The  $\{2, 1, 1\}$  state sheds angular momentum the most efficiently.

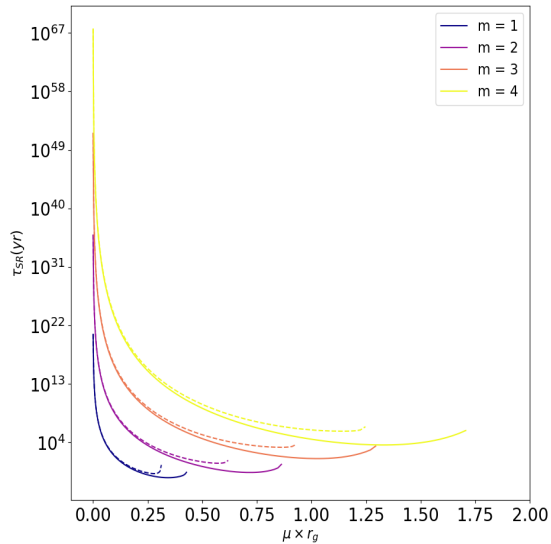


Fig. 15. Superradiant event lifetime for a given BH and boson mass, set by the gravitational fine structure constant  $\alpha = \mu_a \times r_g$ . We use  $M = 10^5 M_\odot$ . Solid lines correspond to  $a^* = 0.99$  and dotted to  $a^* = 0.9$ . Lifetimes are expected to increase proportionally as mass increases, as there will be more angular momentum available for a given effective spin.

Still, we can estimate the spin down lifetime of a BH due to superradiance with Eq. 31. Utilizing the results of [19], the  $\{n, l, m\} = \{2, 1, 1\}$  state is the most efficient at extracting angular momentum. Applying our formula to this superradiant state, we find that the lifetime to spin down from  $a^* = 0.9999$  to  $a^* \approx 0.15$  for a  $M = 10^5 M_\odot$  BH to be roughly  $10^{16}$  seconds. This is approximately  $10^8$  times faster than it takes for a Kerr BH to lose spin due to purely radiative processes. Granted, this is still a rotating BH, but this process serves to greatly reduce the spin and overall lifetime due to the significant influence of effective spin on BH temperature and particle emission rate. In general the lifetime of a BH superradiant event of a BH can be estimated as  $\tau_{SR} = \frac{1}{\Gamma_{SR}}$  [21]. Using our superradiant rates derived from [19], we illustrate the expected lifetime of a given superradiant event for a solar mass BH and variable gravitational fine structure constant  $\alpha = \mu_a M$  in Fig. VI. In general for the  $m = 1$  states available for superradiation, the smaller the gravitational fine structure constant the more effective spin is available to be shed. This is the reasoning for the increase in lifetime as  $\alpha = \mu_a \times r_g$  goes to zero within the figure. Overall, a significant amount of the available spin can be lost from a superradiant event. When considering the lowest superradiant state, all BHs shed spin under approximately  $10^{20}$  seconds, which is significantly faster than the expected Kerr evaporation timescales.

## VII. CONCLUSIONS

This comprehensive study systematically compares the evaporation dynamics of Schwarzschild, Kerr, and Reissner-Nordström black holes through the lens of Page factors, revealing critical insights into the interplay of mass, charge, and angular momentum loss. For **Schwarzschild black holes**,

isotropic Hawking radiation drives mass loss on timescales governed solely by the Stefan-Boltzmann law, with evaporation rates scaling as  $M^{-2}$ . In contrast, **Kerr black holes** exhibit rapid angular momentum dissipation due to preferential emission of high-spin particles and superradiance effects, leading to a spin-down phase orders of magnitude faster than mass loss. This asymmetry arises from frame-dragging effects, which amplify emission from equatorial regions and enhance the coupling of angular momentum to radiation fields.

For **RN black holes**, charge loss dominates early-stage evaporation, mediated by the efficient emission of charged particles through both Hawking radiation and Schwinger pair production. The Coulomb potential barrier introduces a self-regulating mechanism: high charge-to-mass ratios ( $Q_*/M$ ) suppress thermal emission by lowering the black hole temperature, while simultaneously accelerating charge loss via enhanced particle tunneling. Near-extremal configurations ( $Q_* \rightarrow 1$ ) exhibit prolonged lifetimes due to suppressed Hawking temperatures, though quantum corrections destabilize these states over cosmological timescales.

A pivotal finding is the **modification of evaporation hierarchies** by non-Standard Model particle species. Introducing large numbers of uncharged dark matter degrees of freedom shifts the balance between mass and charge loss rates. For example, a dark sector with  $\mathcal{O}(100)$  massless particles can invert the canonical hierarchy, causing  $\dot{M}/M$  to exceed  $\dot{Q}_*/Q_*$  even for highly charged black holes. This challenges assumptions about "charge neutrality" as a universal endpoint of evaporation and suggests that astrophysical black holes in dark matter-rich environments may retain residual charges longer than predicted by SM-only models.

The role of **greybody factors** further complicates these dynamics. For Kerr black holes, frame-dragging distorts emission spectra, favoring low-angular-momentum modes and accelerating spin loss. In RN systems, greybody corrections suppress charged particle emission at low energies but enhance high-energy discharges, creating a feedback loop that regulates charge loss. These effects are particularly pronounced in near-extremal regimes, where geometric optics approximations break down, necessitating full wave-equation treatments for accuracy.

**Schwinger pair production** emerges as a critical mechanism for light ( $M \lesssim 10^{17}$  g), highly charged black holes. At  $Q_*/M \gtrsim 0.5$ , this quantum electrodynamic process dominates over Hawking radiation, ejecting  $e^\pm$  pairs and accelerating charge loss. However, for primordial black holes formed with near-extremal charges, Schwinger emission can transiently \*increase\*  $Q_*$  by preferentially removing opposite charges—a counterintuitive result with implications for early-universe baryogenesis.

**Superradiance** plays a role for any mass BH to extract significant amounts of angular momentum of a Kerr BH in the form of a light boson cloud. For a given BH mass, a range of axion masses allow for  $\Delta a^* = \mathcal{O}(1)$  changes in the overall angular momentum on timescales much faster than that of Hawking radiation. The possibility of forming a gravitational atom allows for much more rapid increases in temperature of the BH and speeds up the overall mass loss of the system as

well.

These results underscore the inadequacy of single-parameter evaporation models and highlight the need for **multivariate frameworks** incorporating particle physics beyond the SM. Future work should explore the interplay between evaporation and accretion in astrophysical environments, quantum gravity corrections to semi-classical approximations, and observational signatures of charged or spinning black holes in gravitational wave or cosmic ray data. Additionally, the discovery that dark sectors can dramatically alter evaporation hierarchies invites experimental tests via high-precision measurements of black hole merger remnants or gamma-ray burst spectra. By bridging thermodynamics, quantum field theory, and astrophysics, this study advances our understanding of black holes as multichannel dissipative systems and provides tools to probe fundamental physics through their evaporation.

## REFERENCES

- [1] S. W. Hawking. Particle creation by black holes. *Communications in Mathematical Physics*, 43(3):199–220, 1975.
- [2] Don N. Page. Particle emission rates from a black hole. i. massless particles from uncharged black holes. *Physical Review D*, 13(2):198–206, 1976.
- [3] Don N. Page. Particle emission rates from a black hole. iii. charged leptons from a nonrotating hole. *Physical Review D*, 16(8):2402–2411, 1977.
- [4] Don N. Page. Particle emission rates from a black hole. ii. massless particles from a rotating hole. *Physical Review D*, 14(12):3260–3273, 1976.
- [5] B. Taylor and W. Hiscock. Evaporation of a kerr black hole by emission of scalar and higher spin particles. *Physical Review D*, 55:6116–6125, 1998.
- [6] Shahar Hod. Hawking radiation may violate the penrose cosmic censorship conjecture. *International Journal of Modern Physics D*, 2019.
- [7] T. Ngampitipan and P. Boonserm. Bounding the greybody factors for non-rotating black holes. *Classical and Quantum Gravity*, 29, 2012.
- [8] R. Dong and D. Stojkovic. Gravitational wave production by hawking radiation from rotating primordial black holes. *Journal of Cosmology and Astroparticle Physics*, 2015.
- [9] Isabella Masina. Dark matter and dark radiation from evaporating kerr primordial black holes. *Gravitation and Cosmology*, 27:134–147, 2021.
- [10] A. Brown and M. Usatyuk. The evaporation of charged black holes. Not Provided, 2024.
- [11] S. W. Hawking and M. Taylor-Robinson. Evolution of near extremal black holes. *Physical Review D*, 1997.
- [12] Don N. Page. Particle emission rates from a black hole. ii. massless particles from a rotating hole. *Phys. Rev. D*, 14:3260–3273, Dec 1976.
- [13] S. W. HAWKING. Black hole explosions? *Nature*, 248(5443):30–31, 1974.
- [14] Alexandre Arbey and Jérémy Auffinger. Blackhawk: a public code for calculating the hawking evaporation spectra of any black hole distribution. *The European Physical Journal C*, 79(8), August 2019.
- [15] Julian Schwinger. On gauge invariance and vacuum polarization. *Phys. Rev.*, 82:664–679, Jun 1951.
- [16] Puxin Lin and Gary Shiu. Schwinger Effect of Extremal Reissner-Nordström Black Holes. Not Provided, 2024.
- [17] Chiang-Mei Chen and Ming-Fan Wu. Spontaneous Pair Production in Reissner-Nordström Black Holes. *Phys. Rev. D*, 85:124041, 2012.
- [18] W. A. Hiscock and L. D. Weems. Evolution of Charged Black Holes. *Phys. Rev. D*, 41:1142, 1990.
- [19] Giovanni Maria Tomaselli. Gravitational atoms and black hole binaries, 2024.
- [20] R. Brito, V. Cardoso, and P. Pani. *Superradiance: Energy Extraction, Black-Hole Bombs and Implications for Astrophysics and Particle Physics*. Lecture Notes in Physics. Springer International Publishing, 2015.
- [21] Asimina Arvanitaki, Masha Baryakhtar, and Xinlu Huang. Discovering the qcd axion with black holes and gravitational waves. *Physical Review D*, 91(8), April 2015.